CHAPTER 16.2
TYPES OF ANTENNAS

William F. Croswell

WIRE ANTENNAS

Analysis of Wire Antennas

The development of wire antennas has been extensive, since such antennas are simple to construct. The classical analysis of wire antennas such as dipoles, loops, and loaded-wire antennas has been developed by Hallen and R. W. P. King and his students; a good summary of theoretical and experimental results, including specific impedance curves and design data, is given in Ref. 1. The unfortunate drawback of this analysis method is that each new wire-antenna configuration presents another analytical problem which must be solved before design computations can be made. A systematic method of solving wire-antenna problems using computerized matrix methods has been developed by extending the analysis of scattering by wire objects by Richmond[2–5] and Harrington.[6–9] These matrix analysis methods have been applied to wire antennas to determine the input impedance, current distribution, and radiation patterns by subdividing any particular wire antenna into segments and determining the mutual coupling between any one segment and all other segments. The method therefore can treat any arbitrary wire configuration, including loading and arrays, the limitation being the storage capacity of available digital computers and the patience of the programmer. In the last 10 years, these numerical methods have been extended to include wire antenna wear obstacles such as towers and mounted on aircraft and missiles.

Wire Antennas over Ground Planes

The wire antenna mounted over a ground plane forms an image in the ground plane such that its pattern is that of the real antenna and the image antenna and the impedance is one-half of the impedance of the antenna and its image when fed as a physical antenna in free space. For example, the quarter-wave monopole mounted on an infinite ground plane has an impedance equal to one-half the free-space impedance of the half-wave dipole. The advantage of the ground-plane-mounted wire antenna is that the coaxial feed can be used without disrupting the driving-point impedance. In practice an antenna mounted on a 2- to 3-wavelength ground plane has about the same impedance as the same antenna mounted on an infinite ground plane. The finite-ground-plane edges produce pattern ripples whose depth and angular extent depend on the ground-plane size.

V Dipole

The V dipole is constructed by bending a wire dipole antenna into a V. The impedance of the half-wave V-dipole antenna has been calculated as a function of the V angle, as given in Fig. 16.2.1. Note that the V dipole is equivalent to the bent-wire monopole antenna over a ground plane. The effect of bending the dipole is to tune

TYPES OF ANTENNAS

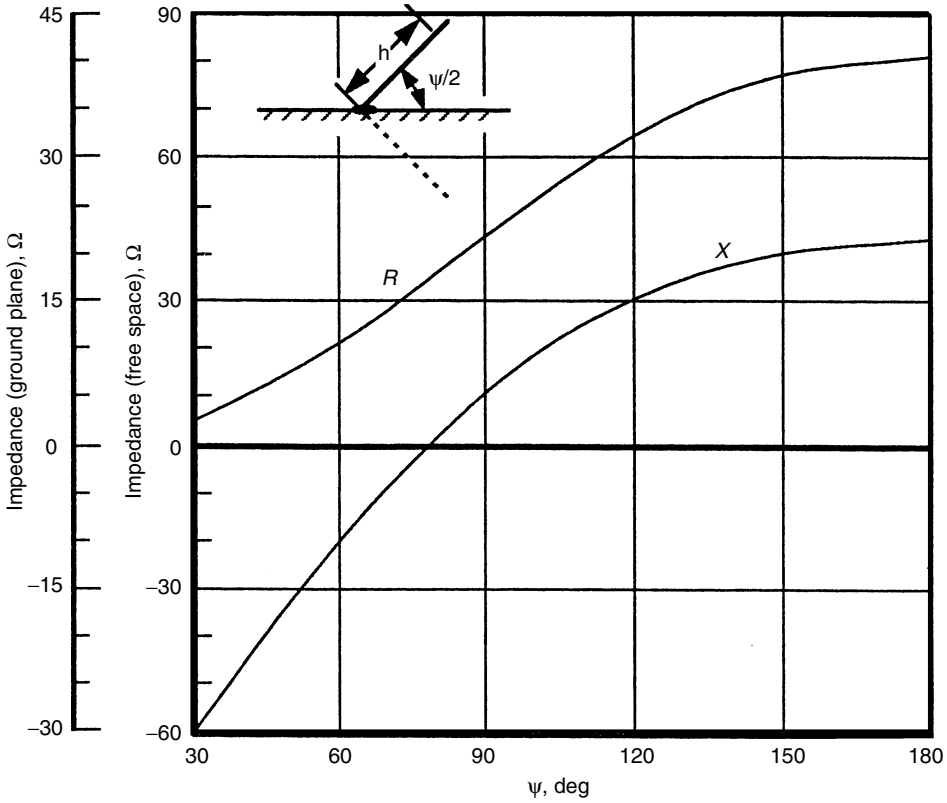

FIGURE 16.2.1 Impedance of a V-dipole antenna as a function of V angle, $h/a = 1000$ n – arm length = $\lambda/4$, a = wire radius. (*Courtesy of J. E. Jones*)

it, giving another practical tuning method in addition to adjusting its length. The patterns of the V dipole (vertical polarization) are nearly identical to those of the straight dipole for φ angles as small as 120°. With decreasing tilt angle this antenna excites a horizontal polarized field component which tends to fill in the pattern, making the antenna a popular communication antenna for aircraft.

Bent Dipole

Another form of the dipole antenna that has practical application, particularly for ground-plane or airplane applications, is the bent-wire dipole formed by bending the wire 90° some distance out from the feed point. The impedance of the bent wire is given in Fig. 16.2.2 for the free-space and ground-plane case. Note that this antenna can also be tuned by adjusting the lengths perpendicular and parallel to the driving point. The radiation pattern in the plane of this antenna is nearly omnidirectional for values of $H_1 \leq 0.10$, after which the pattern approaches that of the vertical half-wave dipole. Other forms of this antenna can be constructed, including loading to reduce the effective length.

Loop Antenna

Another useful classical antenna is the loop antenna. As stated earlier, many investigators have erroneously designated this antenna as a magnetic dipole when indeed it is just another form of the wire antenna.

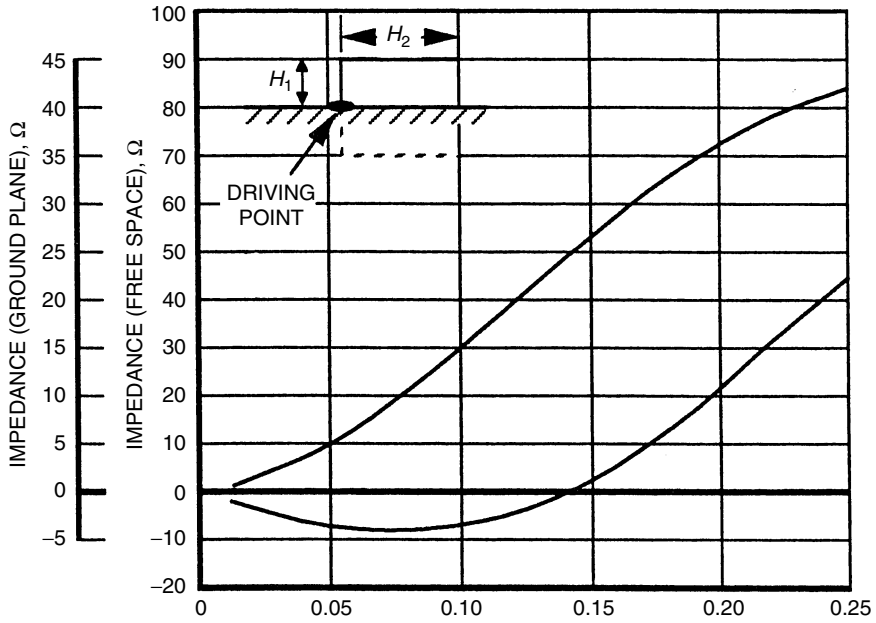

FIGURE 16.2.2 Impedance of half-wave bent-dipole antenna, $H_1 + H_2 = \lambda/4$. (*Courtesy of J. E. Jones*)

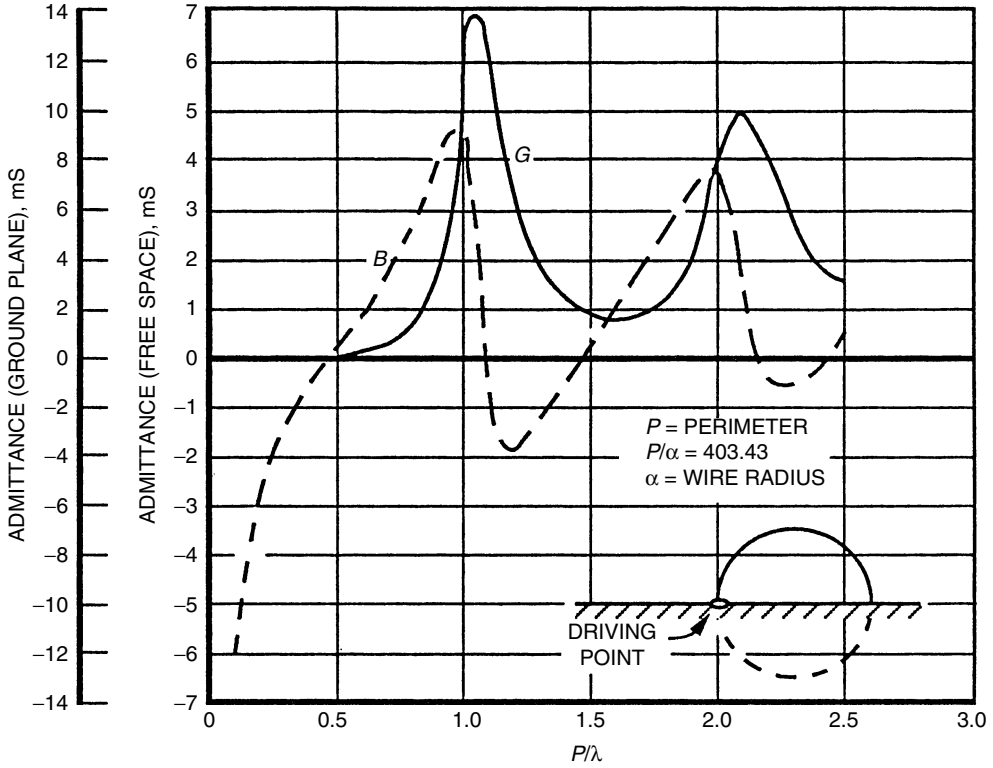

FIGURE 16.2.3 Admittance of the loop antenna. (*Courtesy of J. E. Jones*)

The admittance of the loop antenna can be computed using the matrix method by approximating the loop with a polygon having the same electrical length. The admittance of a 12-sided polygon, which is identical to the admittance of a loop of the same length, has been computed and is given in Fig. 16.2.3. These results have been verified in the ground-plane case experimentally.[10] Indeed the square loop or any other multisided loop with the same electrical-perimeter length has approximately the same admittance as the circular loop. Another method of improving the impedance of a loop is to add turns or load the loop with discrete lumped capacitances. The patterns and impedance of loop antennas mounted on aircraft structures have been studied.

Wire Antennas near Ground Planes

Although the impedance of wire antennas mounted on ground planes several wavelengths in dimension for practical purposes is similar to the impedance of the same antenna mounted on an infinite ground plane, the patterns of wire antennas on finite ground planes strongly depend on the ground-plane size. In recent years, the geometrical theory of diffraction (GTD) has been successfully applied to such problems.[11–16] These published results and the method of analysis are of great interest to antenna engineers since the geometry is the practical one of interest.

Loop above a Finite Ground Plane

The loop above a finite ground plane is an antenna commonly used as an array element in VHF omnirange stations located near all airports as an aircraft landing aid. Since the pattern of the small loop is symmetrical in azimuth, the elevation pattern of a loop over a finite circular ground plane can be computed using a pair of closely spaced line sources fed out of phase and located over a finite-width conducting strip.[14] The geometry of the line-source pair a distance d above a ground plane $2x_0$ in width is shown in Fig. 16.2.4.

The pattern of this antenna has a null at $\phi = 90°$ and a maximum value at some angle above the ground plane, which depends on the spacing d and the ground-plane size $2x_0$. The value of the field along the ground-plane edge ($\phi = 0$) is also of interest to the antenna designer. The variation of these field parameters is given in Fig. 16.2.5.

Horizontal Dipole over a Finite Ground Plane

The GTD method can be applied to the horizontal dipole over a finite ground plane,[15] the geometry of which is shown in Fig. 16.2.6. Also shown in Fig. 16.2.6 is the geometry of the same dipole placed over a cylinder. The purpose of this antenna design is to minimize the ripple or field variation in the pattern above the ground plane and simultaneously achieve a low back-lobe level. These field parameters are plotted as a function of ground-plane size and dipole spacing in Fig. 16.2.7. Also plotted in Fig. 16.2.7 are similar design curves for the dipole spaced the same parametric distances above a perfectly conducting cylinder having a diameter equal to the finite-ground-plane width. These calculations were made by programming available formulas. The cylinder curvature allows one to obtain a better back-lobe level for a given pattern variation or ripple in the forward region. Experimentally, it has been determined that the rear part of the metal cylinder can be substantially removed with little effect.

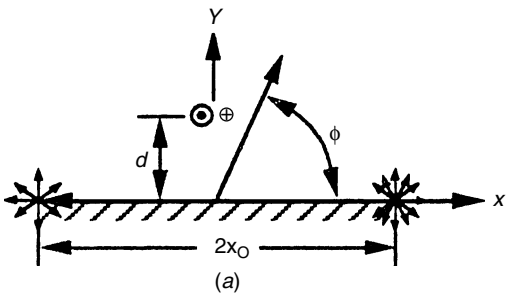

FIGURE 16.2.4 Linear array of line sources and its diffraction mechanism, a two-element array above a ground plane. (*Adapted from Balanis*[14]).

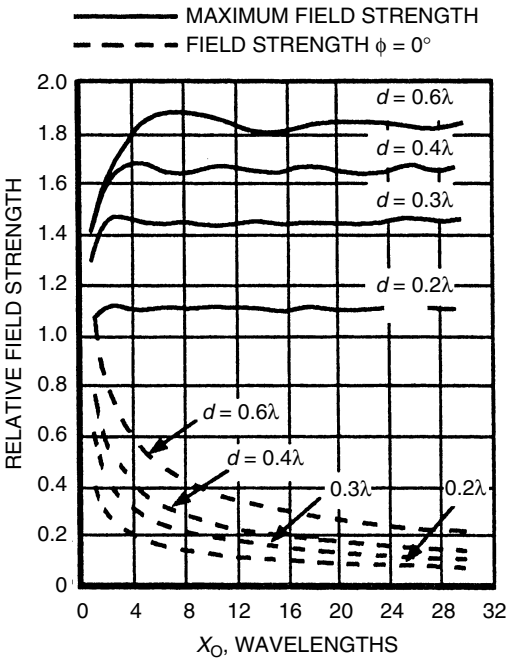

FIGURE 16.2.5 Variations of the maximum field strength and the field strength at the angle of the ground-plane edge as a function of line-source spacing and ground-plane size. (*Adapted from Balanis*[14])

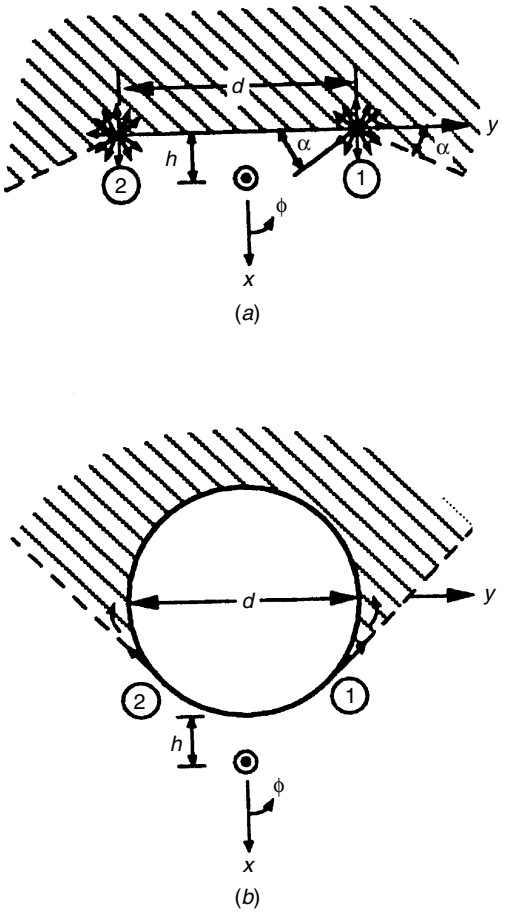

FIGURE 16.2.6 Radiation mechanism of dipole near finite ground plane and circular conducting cylinder. (*a*) ground plane; (*b*) circular cylinder. (*From Balanis and Cockrell*[15])

WAVEGUIDE ANTENNAS

General Considerations

The waveguide antenna, which consists of a dominant-mode-fed waveguide opening onto a conducting ground plane, is very useful for many applications such as a feed for reflector antennas or a flush-mounted antenna for aircraft or spacecraft. For flush-mounting purposes it is sometimes desirable or necessary to cover the ground plane with dielectric layers to protect the aperture from the external environment or in some instances to put dielectric plugs in the feed-waveguide section. The impedance properties of waveguide antennas have been studied extensively both theoretically and experimentally, particularly for the rectangular waveguide, the circular waveguide, and the coaxial waveguide or so-called annular slot. For unloaded apertures, the assumptions of the single-mode trial field in the impedance variational solution has proved adequate for practical purposes. The impedance of these antennas is relatively independent of ground-plane size so long as the ground plane is 2λ in dimension or greater. However, the radiation pattern of the waveguide antenna mounted on finite ground

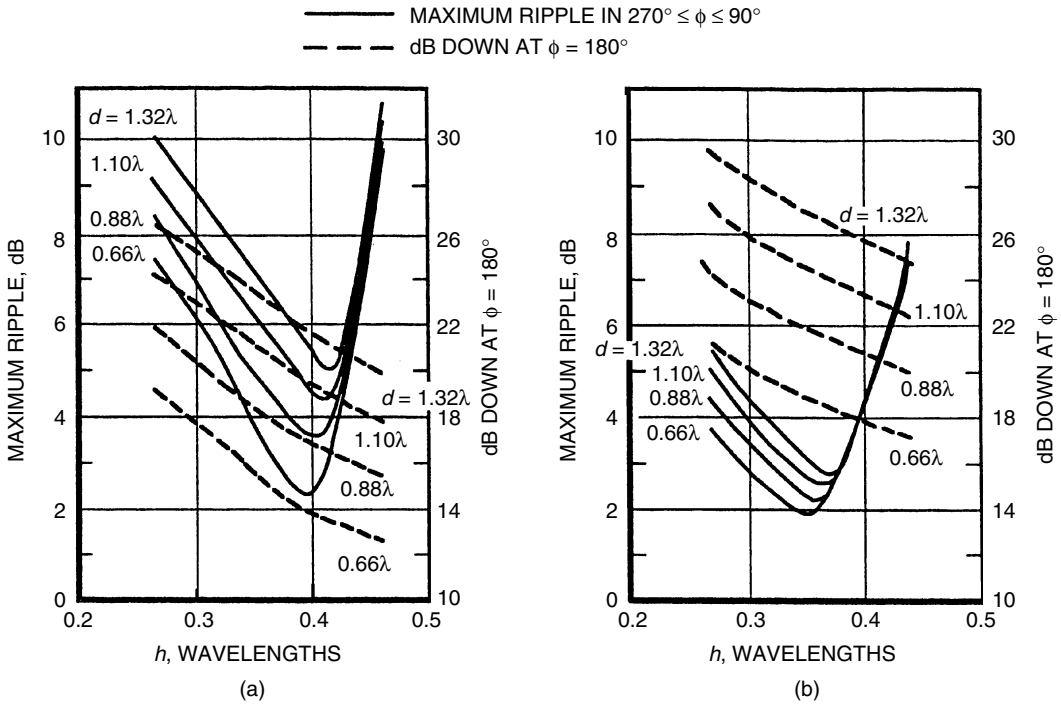

FIGURE 16.2.7 Variations of maximum ripple in $270° \le \phi \le 90°$ region and radiation $\phi = 180°$ as functions of dipole position h near (*a*) the ground plane and (*b*) circular conducting cylinder. (*From Balanis and Cockrell*[15])

planes is very dependent on the ground-plane size. The effects of diffraction by ground-plane edges can be treated by the GTD in a manner similar to that used for wire antennas above a finite ground plane.

Aperture Admittance of Rectangular Waveguides

Calculations have been made assuming the dominant mode as a trial function. These calculations are compared with measured results in Fig. 16.2.8, where the waveguide flange was used as a ground plane. (Note that the *X*-band flange was 1.62 by 1.62 in. and the S-band flange was 6.42 by 6.42 in.) Other measurements were made with up to 10λ ground planes with similar results, as given in Fig. 16.2.8. Calculations of the aperture admittance of square waveguides are given in Fig. 16.2.9. Note that the square waveguide aperture is more nearly matched to the characteristics admittance of the waveguide than the rectangular one. This is also true for the circular aperture.

Aperture Admittance of Circular Waveguides

Calculations for the circular waveguide radiating both into free space and into dielectric slabs have been performed and compared with measurements.[18–19] Calculations for a 1.5 in.-diameter waveguide operating at *C* band are given in Fig. 16.2.10. Note that the circular waveguide is nearly matched when radiating into free space. Like that of the rectangular waveguide, the aperture admittance of the 2λ ground-plane antenna closely approximates the infinite-ground-plane model.

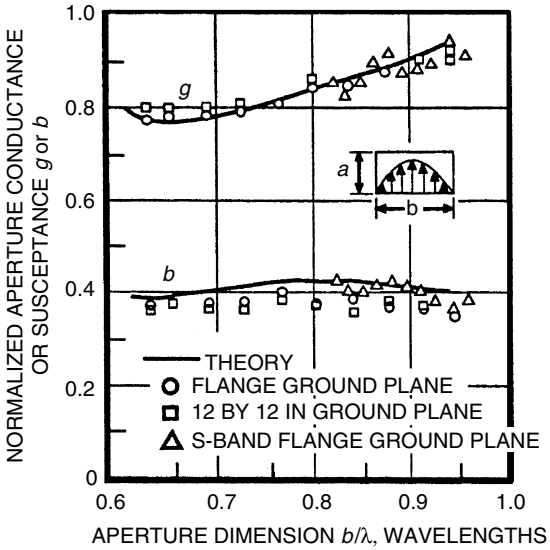

FIGURE 16.2.8 Aperture admittance of a square waveguide.

Patterns of Waveguides on Finite Ground Planes

The design of waveguide antennas on finite ground planes can also be treated by the geometrical theory of diffraction in a manner similar to that for the wire antennas above a finite groundplane. Edge or diffraction effects will primarily occur only in the *E*-plane (*yz* plane) of the circular or rectangular waveguide.

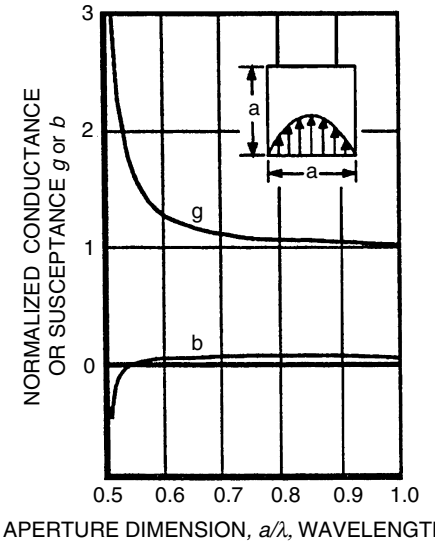

FIGURE 16.2.9 Measured and computed aperture admittance of a circular waveguide. (*From Bailey and Swift*[19])

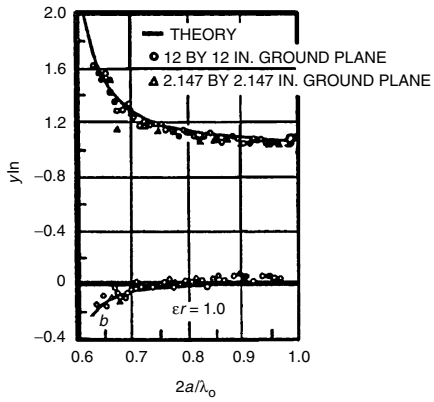

FIGURE 16.2.10 *E*-plane radiation patterns of a TE01-mode-excited rectangular aperture opening onto a finite ground plane vs. aperture size in wavelengths. Ground-plane size = 4λ.

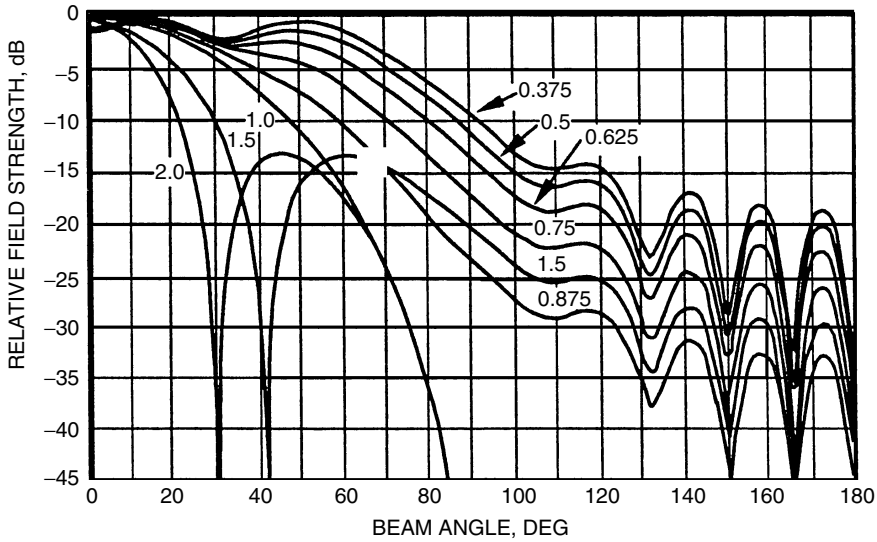

FIGURE 16.2.11 *E*-plane radiation patterns of a TE11-mode-excited circular aperture opening onto a finite ground plane vs. aperture size in wavelengths. Ground-plane size = 4λ.

A summary of calculations for waveguides with different aperture sizes is given in Fig. 16.2.11. The radiation patterns differ for different ground-plane sizes. It should be noted that no diffractions occur in the *E* plane for a 1λ-wide rectangular aperture or a 1.22λ-diameter circular aperture. Indeed, for these aperture dimensions the *E*- and *H*-plane patterns are nearly identical.

The impedance properties of thin-slot antennas are relatively independent of ground-plane size.

Patterns of Narrow Slots in Cylinders

The radiation pattern of a thin circumferential waveguide fed slot on a cylinder is about the same as a similar slot on an infinite ground plane if the cylinder $C = ka$ is greater than about 8.0 to 9.0. The pattern of the axial slot on a cylinder is quite sensitive to the mounting cylinder size, as shown in Fig. 16.2.12.

HORN ANTENNAS

The horn antenna may be thought of as a natural extension of the dominant-mode waveguide feeding the horn in a manner similar to the wire antenna, which is a natural extension to the two-wire transmission line. The most common type of horns are the *E*-plane sectoral, *H*-plane sectoral, and pyramidal horn, formed by expanding the walls of the TE_{01}-mode-fed rectangular waveguide or the conical horn formed by expanding the wall of the TE_{11}-mode-fed circular waveguide. Early work concerned the determination of the forward radiation patterns, directivity, and approximate impedance of sectoral, pyramidal, and conical horns, including comprehensive experimental studies.[21–30] An excellent summary of this work is given by Compton and Collin.[31] In later work, the input impedance, wide-angle side lobes, and back lobes of certain horn antennas have been determined to a high precision using the GTD.[32–36] The remainder of this chapter on horn antenna will follow the work by Milligan[89] and his chapter on horn antennas.

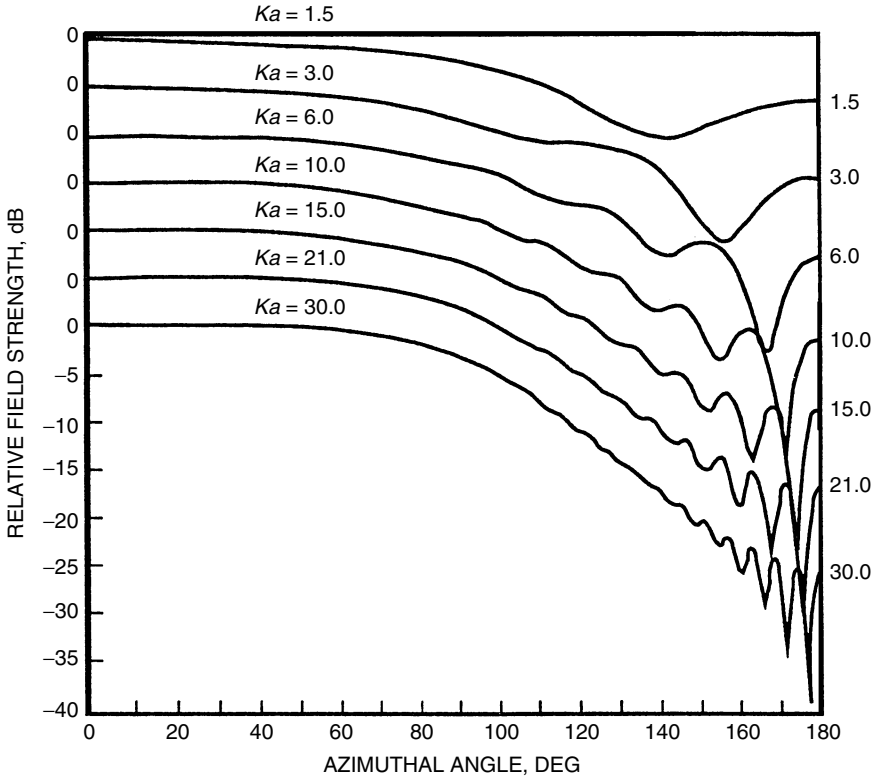

FIGURE 16.2.12 Radiation patterns of an axial infinitesimal slot on a cylinder vs. cylinder circumference *Ka* in wavelengths. Note that the vertical scale for each pattern is displaced 5 dB for clarity.

The general geometry of the waveguide fed horn is given in Fig. 16.2.13. The general phase error in the aperture is given by

$$S = \frac{\Delta}{\lambda} = \frac{\mathrm{W}^2}{8\lambda \mathrm{R}} \tag{1}$$

Sectoral and Pyramid Horns

The general geometry for the pyramidal horn is given in Fig. 16.2.14. For the *E* plane and *H* plane of the sectoral horn, or the *E* and *H* planes of the pyramidal horn, the quadratic phase error can be expressed as

$$S_E = \frac{a^2}{8\lambda\ R_E}, \quad S_H = \frac{b^2}{8\ \lambda R_H} \tag{2a,b}$$

The quadratic phase error change the TE_{10} mode excited horn aperture radiation pattern that is dependent on the amount of phase error S_E and/or S_H. Universal patterns for the sectoral and pyramidal horn are given in Figs. 16.2.15 and 16.2.16.

TYPES OF ANTENNAS

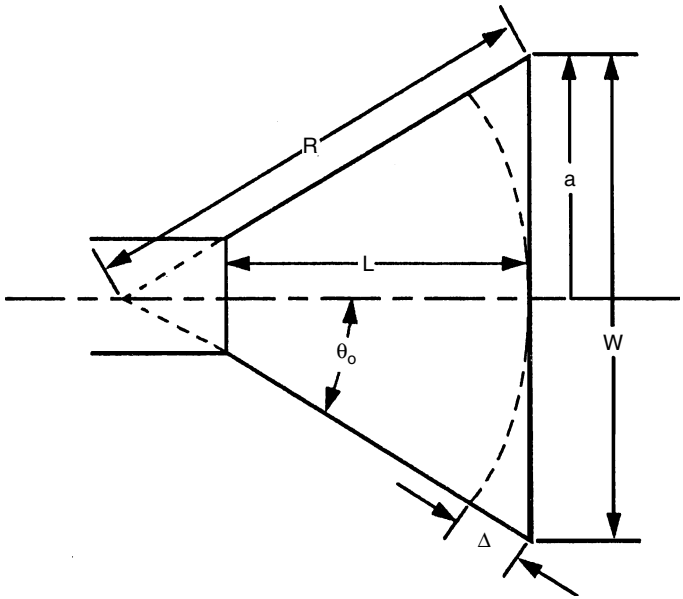

FIGURE 16.2.13 General geometry of a waveguide horn. (*Adapted from Milligan,*[89] *p. 180*)

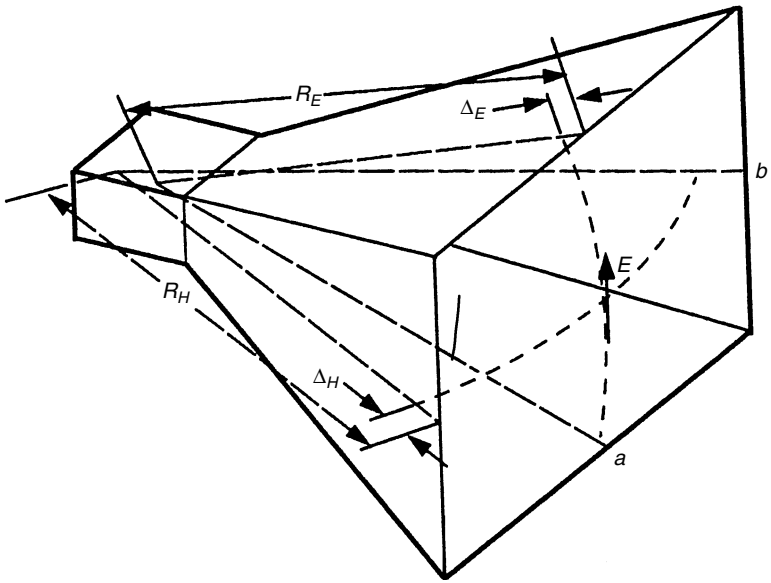

FIGURE 16.2.14 The geometry of a pyramidal horn. (*Adapted from Milligan,*[89] *p. 181*)

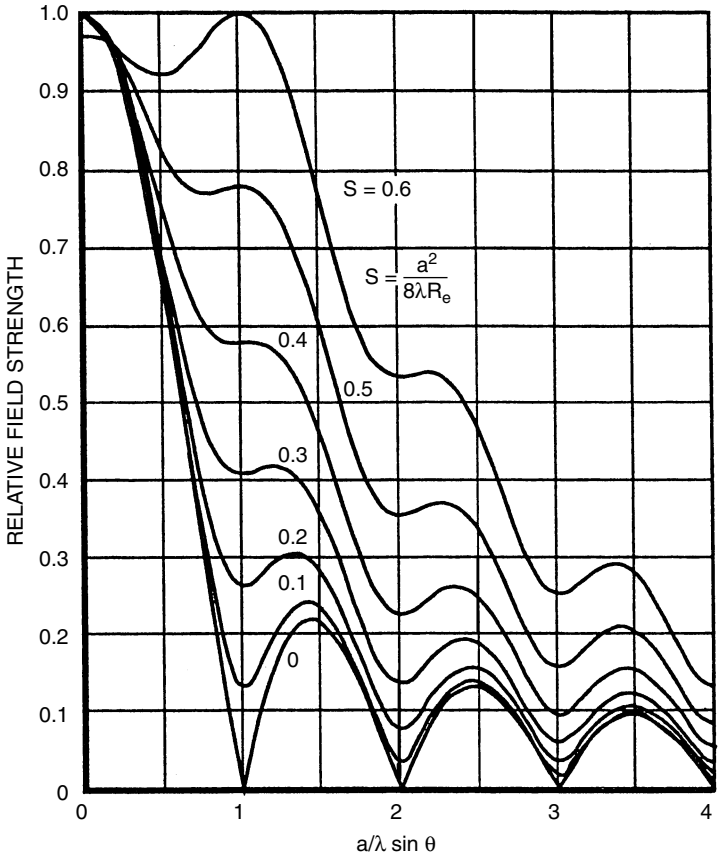

FIGURE 16.2.15 Universal pattern of a pyramidal horn, *E* plane. (*Adapted from Milligan,*[89] *p. 182*)

The gain of pyramidal and sectoral horns has been determined to accuracies of about ±0.4 dB even for frequencies as high as 38 GHz.[37] The most common gain standard is the pyramidal horn, which has a gain equal to

$$\text{Gain}_{\text{dB}} = 10(1.008) + \log a_\lambda\, b_\lambda) - (L_E - L_H) \tag{3}$$

where a_λ, b_λ are aperture dimensions in wavelengths and L_e, L_h are the loss due to phase error in *E* and *H* planes of horn as given in Fig. 16.2.17. Gain curves for other horns and an excellent summary of horn-design information are given by Jakes[38] and Compton and Collin.[31]

Conical Horns

The conical horn formed as an extension of the circular waveguide excited in the TE_{11} mode has been thoroughly studied by King.[29] The radiation patterns of his antenna can be obtained by integrating the dominant TE_{11}-mode field, with quadratic phase error (Fig. 16.2.17). As in rectangular-waveguide-fed horns, the fields outside the aperture are neglected, and therefore, the wide-angle side lobes and back lobes will be computed incorrectly with such a procedure. The universal radiation patterns of conical horns excited by a circular

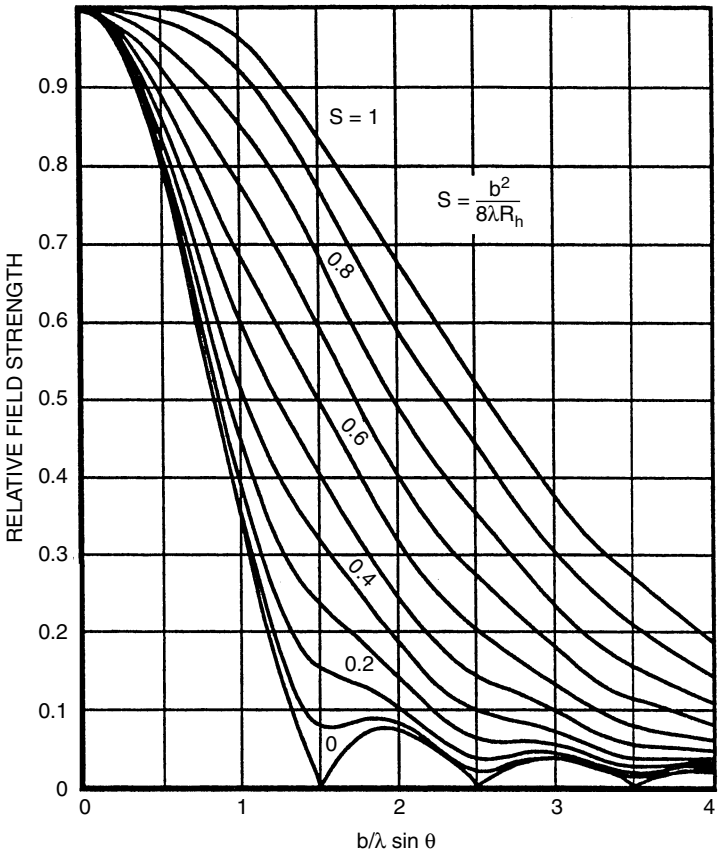

FIGURE 16.2.16 Universal pattern of a pyramidal horn, *H*-plane. (*Adapted from Milligan,*[89] *p. 183*)

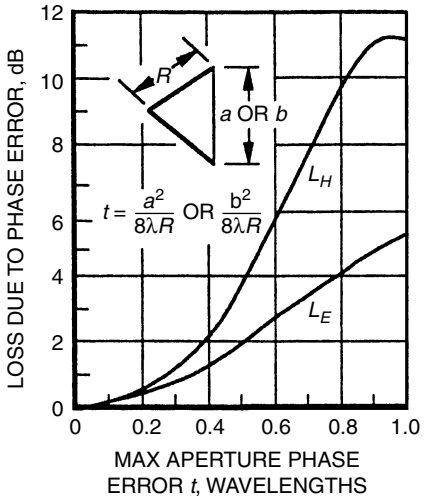

FIGURE 16.2.17*a* Loss correction for phase error in sectoral and pyramidal horns. (*From Jakes*[38])

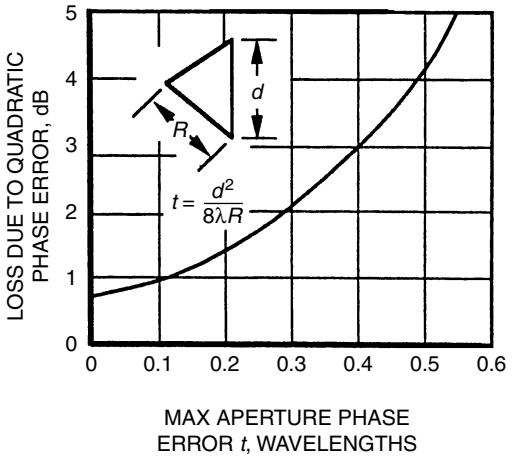

FIGURE 16.2.17*b* Loss correction for phase error in conical horns. (*From Jakes*[38])

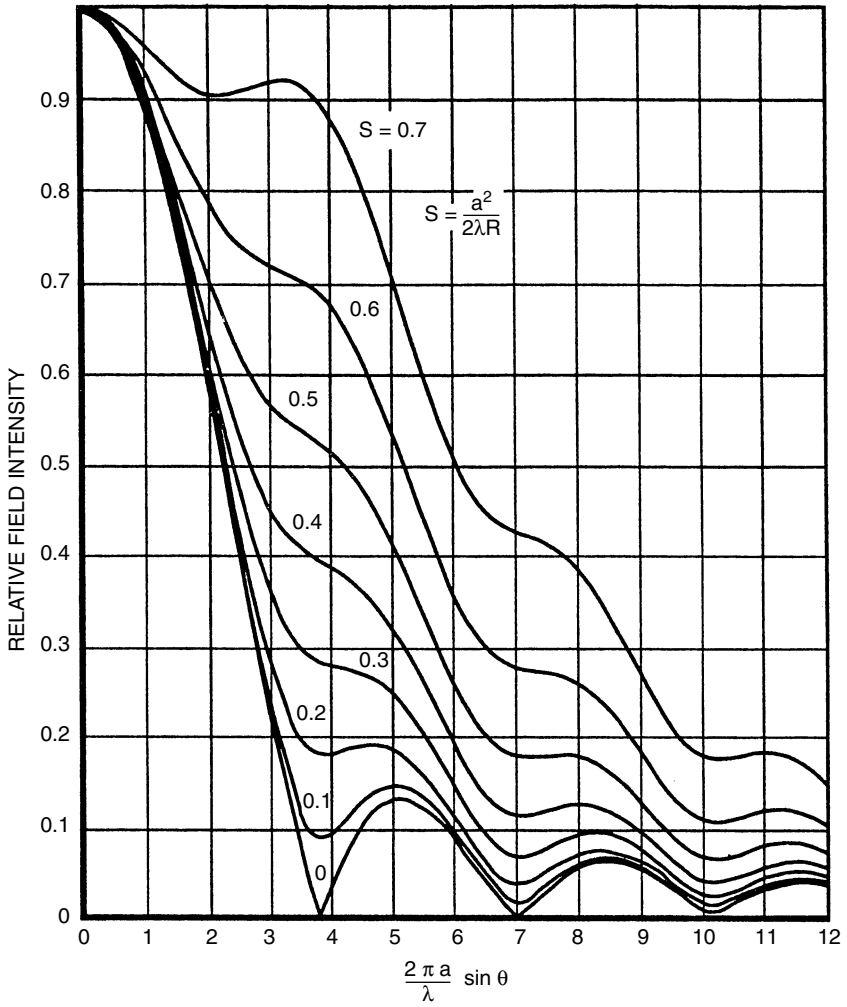

FIGURE 16.2.18 *E*-plane universal pattern of a TE_{11} mode excited conical horn. (*After Milligan,*[89] *p. 192*)

waveguide excited in the TE_{11} dominant mode are given in Figs. 16.2.18 and 16.2.19 for various values of quadratic phase error. Care must be used in exciting this horn since any feed asymmetry may excite the TM_{01} mode in the feed waveguide.

The gain of the conical horn has been determined to be

$$\text{Gain}_{\text{dB}} = 20 \log C\lambda - L \tag{4}$$

where C is the circumference of horn aperture and L is the gain loss due to phase error given by curve in Fig. 16.2.17. It should be carefully noted that the gain given by Eqs. (3) and (4) neglects the losses in the conducting walls of the entire horn and the VSWR.

TYPES OF ANTENNAS

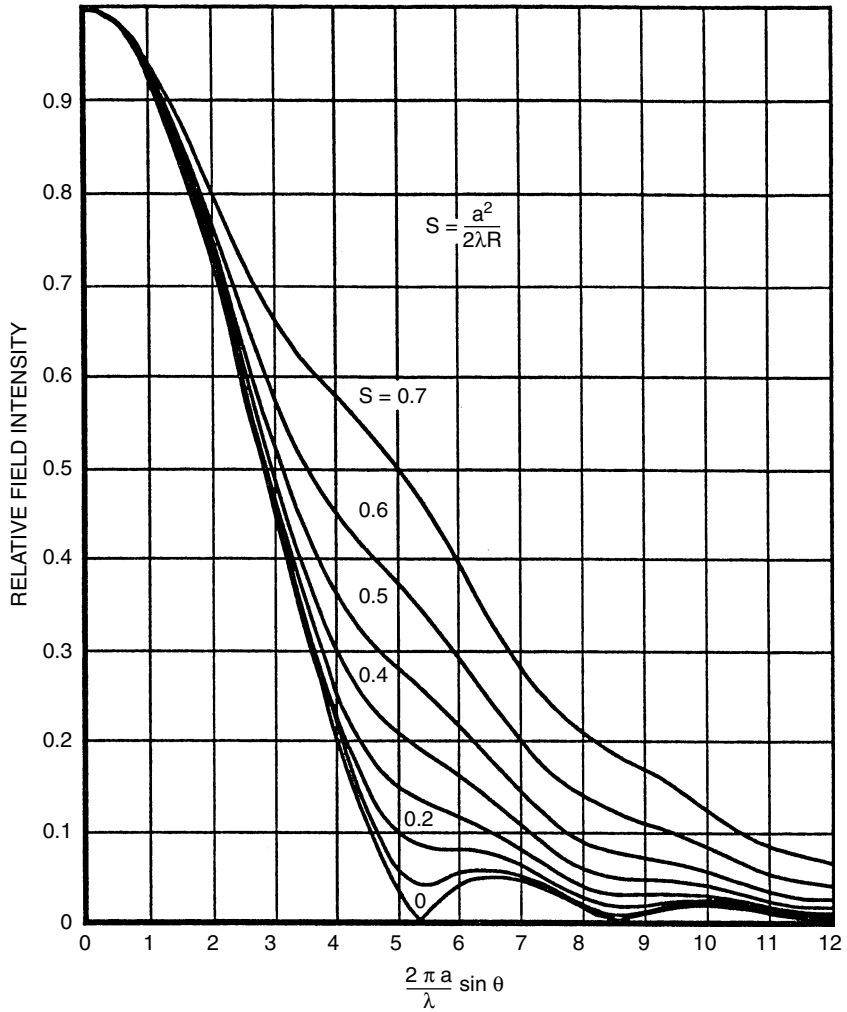

FIGURE 16.2.19 *H*-plane universal pattern of a TE_{11} mode excited conical horn. (*After Milligan,*[89] *p. 193*)

Corrugated Horns

The conical horn can have undesired pattern ripples, particularly in the *E* plane. Such patterns are undesirable for horn feeds used in high-efficiency parabolic antennas. The most commonly used horn feed is the corrugated conical horn described[39] in Fig. 16.2.20. The teeth in these horns generally are between $\lambda/4$ and $\lambda/2$ deep, although the best operating band is about 1.5 to 1. These horns convert the dominant waveguide feed TE_{11} mode into the hybrid HE_{11} which tend to make the *E*-plane pattern similar to the H-plane pattern. Therefore, the narrow angle corrugated horn (10 dB beamwidth, less than 74°) has a very symmetrical pattern in the ϕ plane as given in Fig. 16.2.21. The so-called scalar horn is of sufficiently wide angle that the phase center is at the horn throat. This horn is particularly useful for wideband applications.[40]

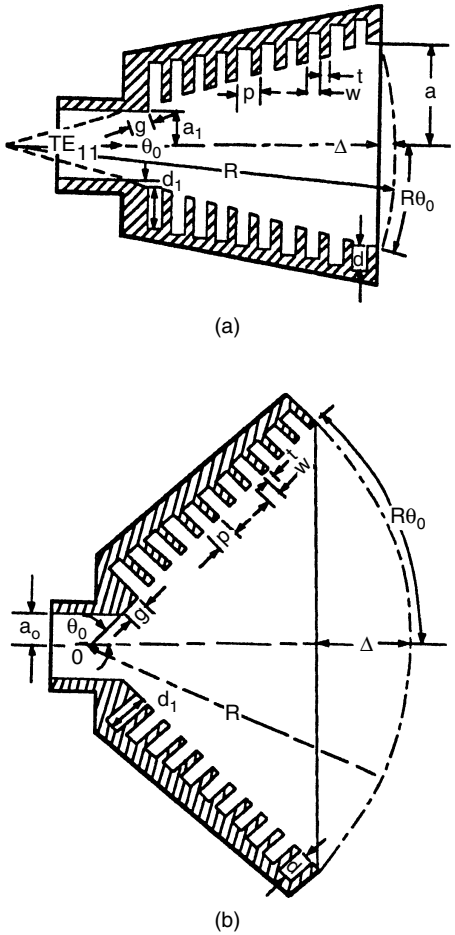

FIGURE 16.2.20 (*a*) Corrugated horn and (*b*) Scalar horn. (*After Milligan*[89] *and Thomas*[39])

REFLECTOR ANTENNAS

The theory commonly used for the direct-fed parabolic antenna is that of Silver,[41] using physical optics. As outlined by Silver, this theory is adequate to predict the gain, radiation pattern, and the level of the first few side lobes of the secondary pattern, neglecting blockage and scattering by feed struts. The effect of feed-strut blockage can be estimated using geometrical optics;[42] however, an analysis of the diffraction of struts using a more rigorous formulation is necessary to improve the quantitative understanding of the problem. The radiation-pattern characteristics of the offset-fed parabola have been determined approximately using an extension of Silver's formulation to include this geometry.[43–44]

The spherical reflector is a good design for a scanning reflector antenna—thanks to its geometrical symmetry; however, a point source at the focal region will not produce a set of parallel rays from the secondary reflector. To correct this spherical-aberration error a line-source feed is employed.[45–46] By phasing this line source, the beam can be scanned to other positions.

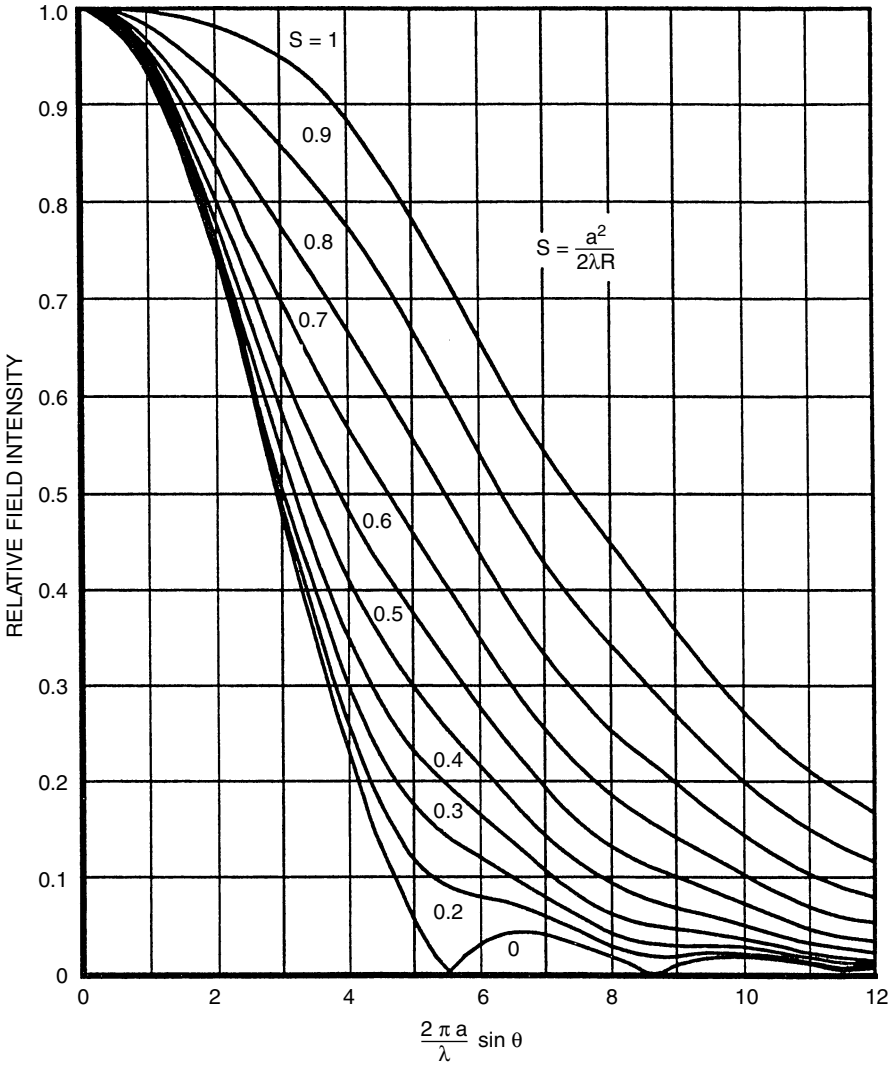

FIGURE 16.2.21 Universal pattern of a conical corrugated horn, HE_{11} mode. (*After Milligan*[89])

Another way of feeding the parabolic reflector antenna is to use a subreflector in the focal region of the parabola and illuminate the subreflector from the parabolic surface. The principal advantages of the Cassegrain system or other methods of folded optics are the increase in effective *f*/*d* ratio and the simple mechanical location of the feed so that cooled receivers used with such antennas can be serviced in a more practical manner. The chief disadvantage is the aperture blockage of the subreflector, which restricts the application of this principle to large aperture. The Cassegrain antenna has been analyzed extensively, and computer programs are available. This design effort resulted in the design and construction of the 210-ft dish antenna[47–56] used in the worldwide space-receiving network. In order to achieve all-weather operating capability a precision 120 ft Cassegrain dish under a 150-ft radome has been constructed at Millstone Hill, Massachusetts. The radome produces about 1- to 2.8-dB loss in the microwave to millimeter-wavelength region.[58]

Besides ground-based antennas, special reflector types for use as erectable spacecraft antennas have been developed. Analysis of the gored reflector[59] is available, as is the design of conical-reflector antenna.[60]

Performance of Symmetric Parabolic Antennas

The purpose of this section is to present a brief summary of the performance of symmetric parabolic antennas in terms of geometric and performance parameters. The information follows the excellent work of Knop[61] and Milligan.[89] Consider the geometry given in Fig. 16.2.22. This figure depicts a feed located at the focal point of a symmetric parabola. The feed illuminates the reflecting surface, so that the secondary radiation pattern is obtained by integrating the surface current until the edge of the dish is reached. (This edge field or edge taper is a design parameter that affects the secondary pattern and gain performance.) Assuming that the feed pattern is symmetrical in both the *E* and *H* planes, a set of universal design curves can be generated as given in Fig. 16.2.23. These data are presented as a function of edge taper in dB. The data plotted in Fig. 16.2.24 is defined in the following manner:

η_B = beam efficiency, which is the percent of the horn energy captured by the parabolic dish antenna
η_A = total aperture efficiency
$\eta A_I = \eta A/\eta B$ = aperture illumination efficiency
$2\theta_3 D/\lambda$, degrees = product of the aperture diameter in wavelengths, multiplied by the full half power beamwidth in degrees ($2\theta_3$)
FSL, dB down = first sidelobe level in dB down from the main lobe peak
$U_{FSL} = \pi(D/\lambda)\sin\theta_{FSL}$ = universal angle at which the first sidelobe occurs.

Other performance parameters are given in Fig. 16.2.23. For example:

(a) amount of phase error loss due to axial defocus $\pm DZ/\lambda$ for various f/D ratios

(b) phase error loss for phase center differential for different f/D ratios

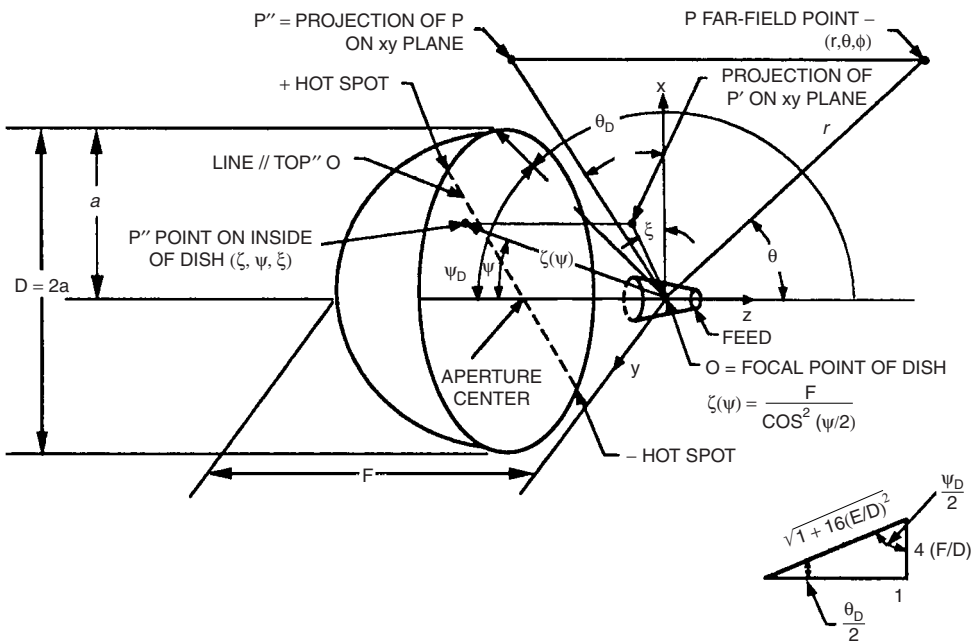

FIGURE 16.2.22 Geometry of a symmetric parabolic dish antenna. (*After Knop*[61])

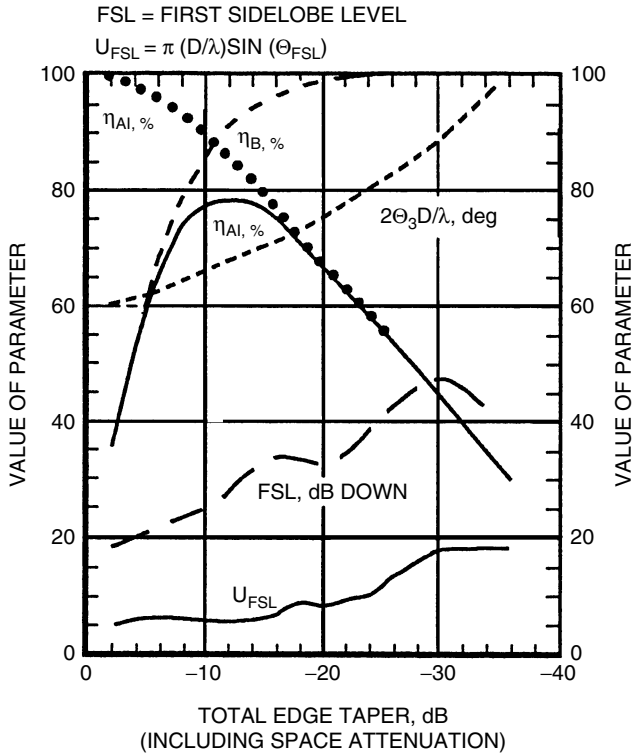

FIGURE 16.2.23 Universal performance curves for a symmetric parabolic dish antenna fed with a feed having symmetrical radiation pattern. (*After Knop*[61])

(c) scan loss versus beamwidths of scan for different *f/D* ratios

(d) beam deviation factor as a function of *f/D* ratio.

The most important performance parameter, the gain loss as a function of the surface roughness, is given in Fig. 16.2.25.

LOG-PERIODIC ANTENNAS

The Frequency Independent Antenna

The frequency independent antenna is specified only by angles. It was suggested by Rumsey[62] in 1954. The simplest form of such antennas is the equiangular spiral,[63] although early models with the frequency-independent idea included the tapered helix.[64–65] All antenna shapes that are completely specified by angles must extend to infinity; thus any physically realizable frequency-independent antenna has bandwidth limitations because of end effects. A simple modification of the frequency-independent antenna is the logarithmically periodic antenna,[66] whose properties vary periodically with the logarithm of the frequency. This modification tends to minimize the end effect, although the impedance will vary as a function of frequency; such variations are sometimes small. From these early designs a number of log-periodic antennas have been developed, including conical log spirals,[67] the log-periodic V,[68] the log-periodic dipole,[69–70] and the log-periodic Yagi-Uda array.[71]

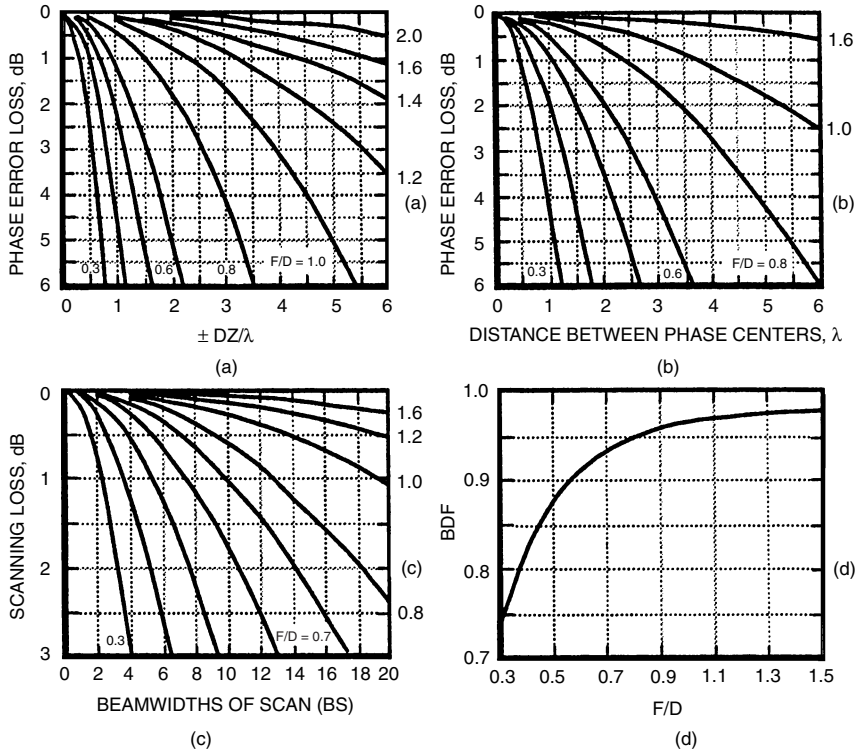

FIGURE 16.2.24 Performance parameters for a symmetrical parabola dish antenna: (*a*) Gain loss due to phase error caused by axial defocusing; (*b*) Gain loss due to the difference between *E*-plane and *H*-plane phase errors; (*c*) Gain loss due to feed scan; and (*d*) the beam deviation factor vs. *f*/*D* ratio.

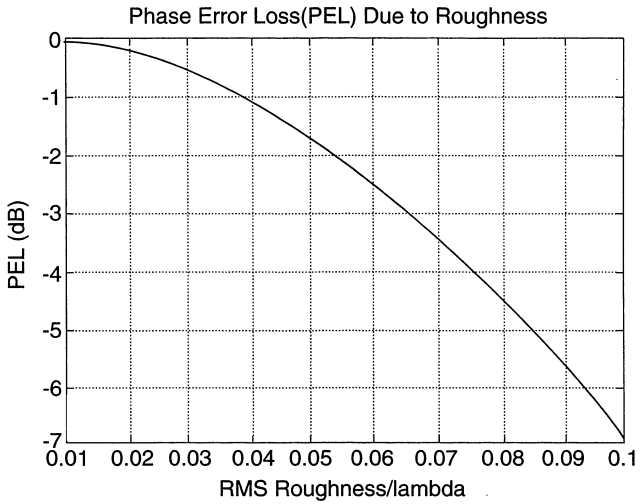

FIGURE 16.2.25 Gain loss due to random RMS error (PEL = −685.8. (RMS Roughness)^2, db).

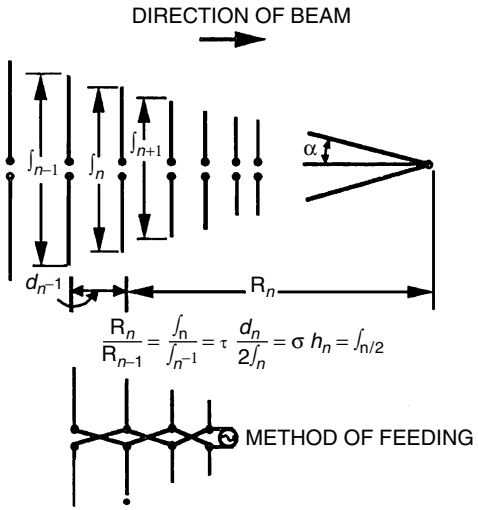

FIGURE 16.2.26 The log-periodic dipole antenna with definition of parameters. (*From Carrel*[70])

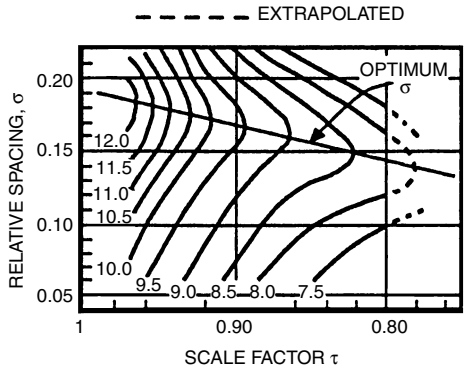

FIGURE 16.2.27 Constant-directivity contours in decibels versus τ and σ. Optimum indicates maximum directivity for a given value of τ. $Z_0 = 100\ \Omega$, $h/a = 100$, $Z_\Gamma = 100\ \Omega$.

Log-Periodic Dipole Design

One of the most popular antennas of this type is the log-periodic dipole antenna, which has the geometry depicted in Fig. 16.2.26. This antenna can be fed either by using alternating connections to a balanced line, as indicated in Fig. 16.2.26, or by a coaxial line running through one of the feeders from front to back. A simple procedure determined by Carre[70] which can be used for designing this antenna is outlined here. The number of elements is primarily determined by τ, and the antenna size is determined by boom length, which depends primarily on σ. The procedure is as follows:

1. An estimate of τ and σ based on the desired gain can be obtained from Fig. 16.2.27.
2. The bandwidth of the structure B_s is given by $B_s = B\,B_{ar}$ where B is the operating bandwidth and B_{ar} is determined in Fig. 16.2.28 using the parameter $\tan \alpha = (1 - \Gamma)/4\sigma$.
3. The length of the first elements is always made $\lambda_{max}/2$, so that the boom length L between the largest and smallest elements can be found from $L/\lambda_{max} = 1/4(1 - 1/B_s) \cot \alpha$.
4. The number of elements required is given by $N = 1 + [(\log B_s)/\log(1/\tau)]$.

By several iterations of this design procedure a minimum boom length can be obtained. The relative feeder impedance of the design can be found using available data.[70]

SURFACE-WAVE ANTENNAS

General Description

A wide class of *surface-wave antennas* has been devised, e.g., the Yagi, backfire, helix, cigar, and polyrod antenna. The surface-wave nomenclature is related to the idea that these antennas, if infinite in length, will support a wave that travels along the structure at a velocity slower than the velocity of light in free space. Data for the phase velocity along such antenna structures are available.[72–74] If the parameters of the antenna structure are chosen so

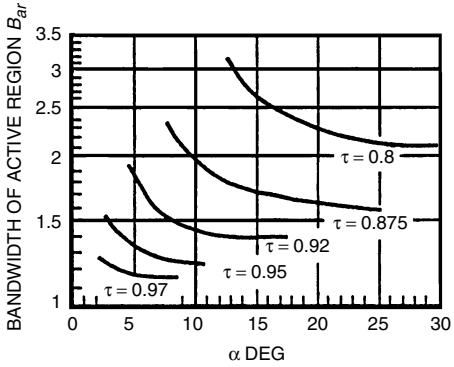

FIGURE 16.2.28 Bandwidth of active region B_{ar} vs. for several values of, for $Z_0 = 100\ \Omega$, $h/a = 125$. (*From Carrel*[70])

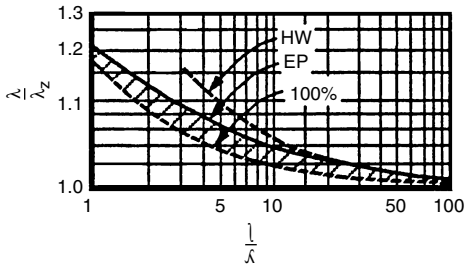

FIGURE 16.2.29 Relative phase velocity $c/v = \lambda/\lambda_z$ for maximum-gain surface-wave antennas as a function of relative antenna length $1/\lambda$. HW = Hansen-Woodward condition; EP = Ehrenspeck-Poehler experimental values; 100 percent = idealized perfect excitation. (*From Zuckel*[75])

that the resultant phase velocity causes the Hansen-Woodward condition to be met on the finite length of the antenna, an increased or supergain condition occurs. The relative phase velocity $c/v = \lambda/\lambda_z$ to maximize the gain as a function of antenna length is given in Fig. 16.2.29. A typical phase-velocity variation as a function of specific antenna parameters is given in Fig. 16.2.30 for the Yagi. Choosing particular antenna parameters so that the optimum phase-velocity conditions are met will result in a good first-cut design. Improved designs require extensive parametric experimental studies where the antenna elements are varied about the initial dimensions. An estimate of how much gain can be expected from surface-wave antennas is given in Fig. 16.2.31. An excellent summary of surface-wave antenna design and literature has been compiled by Zucker.[75,76]

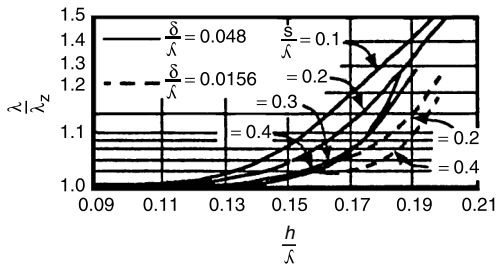

FIGURE 16.2.30 Relative phase velocity on a Yagi antenna (data from Ehrenspeck and Poehler and Frost); δ = diameter of wire element, s = spacing between elements, and h = half length of element. (*From Zucker*[76])

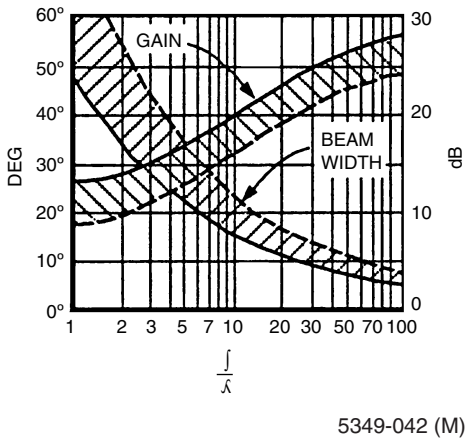

FIGURE 16.2.31 Gain and beam width of surface-wave antenna as a function of a relative antenna length $1/\lambda$. For gain (in decibels above an isotropic source) use right-hand coordinate; for beam width left-hand coordinate. Solid lines are optimum values; dashed lines are for low-side-lobe and broadband design. (*From Zucker*[76])

TYPES OF ANTENNAS

The surface-wave antenna is a misnomer since surface waves do not exist on finite antennas. Consequently, aside from the use of the general concepts mentioned above, most surface-wave antennas are designed experimentally because of the importance of the feed radiation and end effects.

Use of Feed Shields

Nearly all surface-wave antennas suffer from side-lobe and beam asymmetry if not fed from special launchers. For example, the helix mounted on a flat ground plane has pattern asymmetry and poor axial ratio (about 3 dB) on axis.[77] Short helices in particular have been found to exhibit this property. A way to improve this helix performance is to use a conical feed shield and to taper the beginning and end turns as in the helicone antenna.[78] The feed shield that improves the performance of the cigar antenna is a conical horn[79] or a square cavity or bucker.[80]

MICROSTRIP ANTENNAS

General Considerations

In many applications where low-profile antennas are required and bandwidths less than a few percent are acceptable microstrip antennas may have the desired characteristics. Microstrip antennas are constructed on a thin dielectric sheet over a ground plane using printed-circuit-board and photo-etching techniques. The most common board is dual-copper-coated Teflon-fiberglass as it allows the microstrip antenna to be curved to conform to the shape of the mounting surface. The antenna itself may be square, rectangular, round, elliptical, and the like; the two most common elements (rectangular and round) are illustrated in Fig. 16.2.32. Circular-polarized radiation can be obtained by exciting the square or round element at two feed points 90° apart and in phase quadrature. Circular polarization can also be obtained over a limited frequency range by making the element slightly rectangular ($W/L \approx 1.03$) or slightly elliptical (eccentricity ≈ 0.2) and using a single feed point on the 45° diagonal.

Resonant Frequency

The frequency response for the basic elements (rectangular or round) is similar to a resonant tuned circuit or cavity. When viewed as a thin cavity, the rectangular element should be resonant when the length is equal to a half wavelength, and the round element should be resonant when the radius is equal to 0.293 wavelength; however, owing to fringing fields at the edges of the element, the actual resonant size is smaller by a few percent, that is, $L_e = 0.5\lambda_e$ and $\alpha_e = 0.23\lambda_e$ where the effective length L_e and effective radius α_e are given by

$$L_e = L + 0.824h[(\epsilon_e + 0.3)/(\epsilon_e - 0.258)][(\alpha L + 0.262h)/(\alpha L + 0.813h)] \tag{5}$$

$$\alpha_e = a[1 + 2h(\pi\alpha\epsilon_r)^{-1} \ln(9.246a/h)]^{1/2} \tag{6}$$

where $\alpha = W/L$, and

$$\epsilon_e = 0.5\ (\epsilon_r + 1) + 0.5(\epsilon_r - 1)(1 + 12h/\alpha L)^{-1/2} \tag{7}$$

The resonant size (for minimum VSWR) decreases for an increase in the thickness h, as shown in Fig. 16.2.33 for the square ($W = L$) and in Fig. 16.2.34 for the round element. The resonant length of the rectangular element also decreases with an increase in the width.[81] A TE-excited strip provides a lower bound on the resonant length of rectangular elements with a large width-to-length ratio.

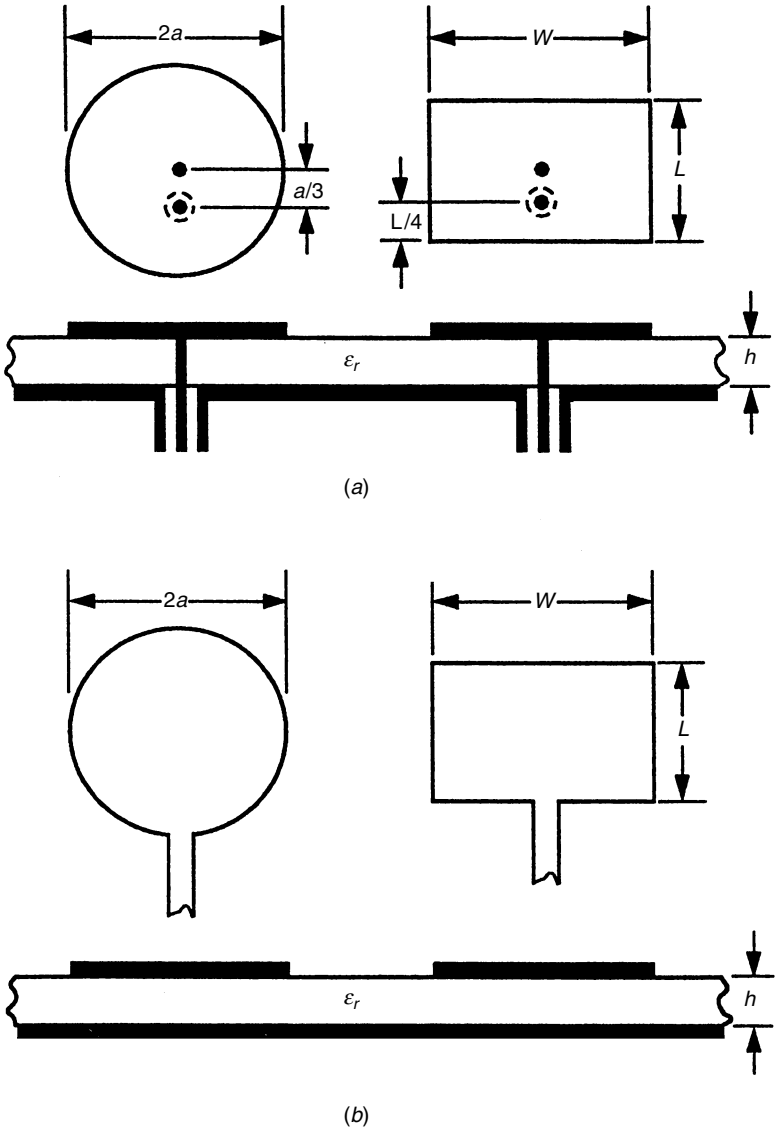

FIGURE 16.2.32 (*a*) Coaxial-fed microstrip antennas; (*b*) line-fed microstrip antennas.

Bandwidth

The bandwidth of microstrip antennas is determined primarily by the thickness of the dielectric, increasing with an increase in thickness, as shown in Fig. 16.2.35 for square and round elements on Teflon-fiberglass with coaxial feed probes. The data in Fig. 16.2.35 can be used to select a board thickness to meet the bandwidth requirement, and the resonant size of the element is then determined for this thickness by using the effective length or radius described earlier.

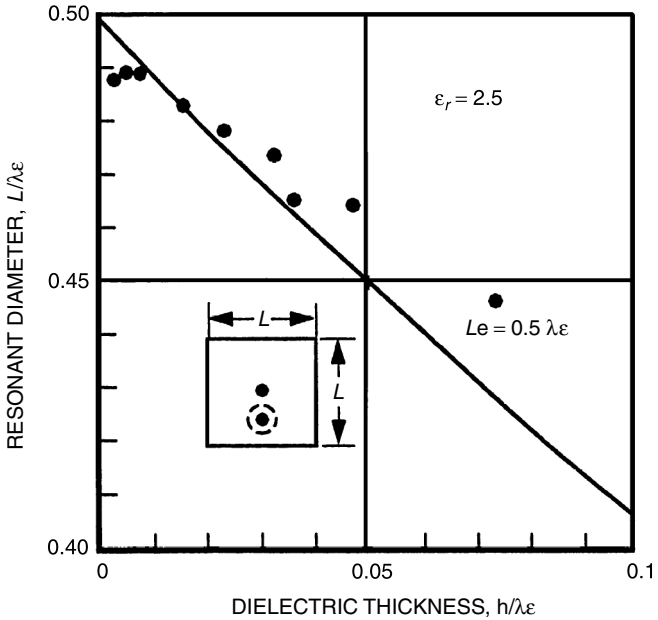

FIGURE 16.2.33 Resonant size of square microstrip antenna.

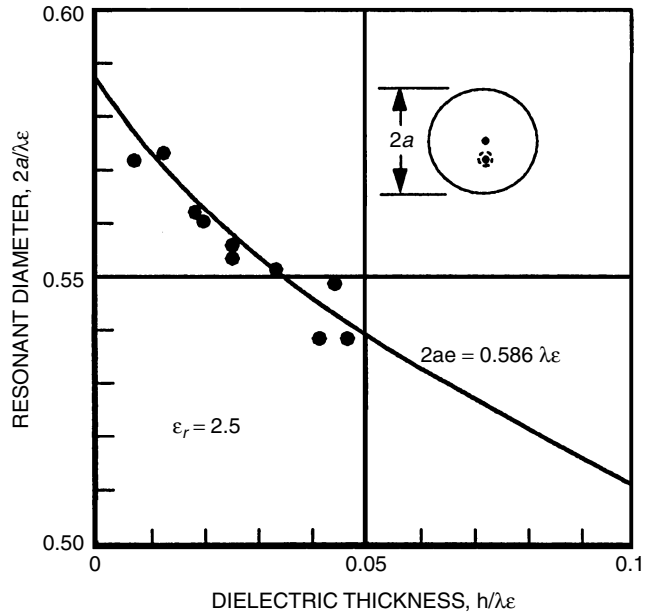

FIGURE 16.2.34 Resonant diameter of round microstrip antenna.

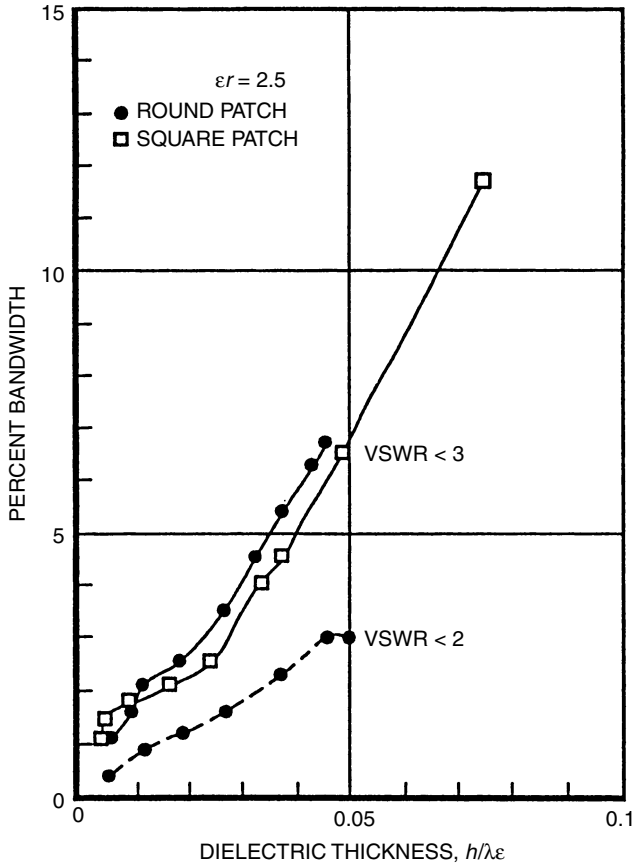

FIGURE 16.2.35 Measured bandwidth for coaxial-fed microstrip antenna.

Impedance

The resonant input impedance for a feed line connected at the edge of a microstrip antenna is about 120 Ω for the rectangular and about 300 Ω for the round element. A quarter-wave section with a characteristic impedance of 77.5 or 122.5 Ω can be inserted in the microstrip feed line to match the rectangular or round element to 50 Ω. In coaxial probe-fed microstrip antennas, the resonant input impedance varies from zero to the center of the element to about 120 Ω (rectangular) or 240 Ω (round) to the edge; therefore, a probe position can always be found, which matches the antenna to the 50 Ω coaxial feed. The exact probe position for a 50 Ω match depends on the thickness of the dielectric; however, it has been found that a coaxial probe positioned *L/4* from the edge of a rectangular element or *a*/3 from the center of a round element will usually yield an input impedance quite close to 50 Ω. Approximate analytical models are also available[81–86] for calculating the impedance of microstrip antennas.

Radiation Patterns

The radiation patterns of round or rectangular microstrip elements can be found from a complementary-waveguide-fed aperture of the same size as the effective size of the microstrip antenna[87] or from slots located around the perimeter of the element.[88]

REFERENCES

1. King, R. W. P. Cylindrical Antennas and Arrays, in R. E. Collin and F. J. Zucker (eds.), "Antenna Theory," Pt. I, pp. 352– 420, McGraw-Hill, 1969.
2. Richmond, J. H. Scattering by an Arbitrary Array of Parallel Wires, *Ohio State Univ. Antenna Lab., Rep.* 1522–1528, Contract N123 (1953)-31663A, April 1964.
3. Richmond, J. H. Scattering by an Arbitrary Array of Wires, *IEEE Trans. Microwave Theory Tech.*, July 1965, Vol. MTT-13, pp. 408–412.
4. Richmond, J. H. A Wire-Grid Model for Scattering by Conducting Bodies, *IEEE Trans. Antennas Propag.*, November 1966, Vol., AP-14, pp. 782–786.
5. Richmond, J. H. Scattering by Imperfectly Conducting Wires, *IEEE Trans. Antennas Propag.*, November 1967, Vol. AP-15, pp. 802–806.
6. Harrington, R. F. Theory of Loaded Scatterers, *Proc. IEEE*, April 1964, Vol. 111, pp. 617–628.
7. Harrington, R. F., and J. Mautz Matrix Methods for Solving Field Problems, *Syracuse Univ. Rep.* RADC TR-66-351, Vol. II, August 1966.
8. Harrington, R. F. Matrix Methods for Field Problems, *Proc. IEEE*, February 1967, Vol. 55, pp. 136–149.
9. Harrington, R. F. "Field Computation by Moment Methods," Macmillan, 1968.
10. Richards, G. A. Reaction Formulation and Numerical Results for Multiturn Loop Antennas and Arrays, Ph.D. dissertation, Ohio State University, 1970.
11. Sengupta, D. L., and V. H. Weston Investigation of the Parasitic Loop Counterpiece Antennas, *IEEE Trans. Antennas Propag.*, March 1969, Vol. AP-17, pp. 180–191.
12. Sengupta, D. L., and J. E. Ferris On the Radiation Patterns of Parasitic Loop Counterpoise Antennas, *IEEE Trans. Antennas Propag.*, January 1970, Vol. AP-18, pp. 34–41.
13. Balanis, C. A. Radiation Characteristics of Current Elements near a Finite-Length Cylinder, *IEEE Trans. Antennas Propag.*, May 1970, Vol. AP-18, pp. 352–359.
14. Balanis, C. A. Analysis of an Array of Line Sources above a Finite Groundplate, *IEEE Trans. Antennas Propag.*, March 1971, Vol. AP-19, pp. 181–185.
15. Balanis, C. A., and C. R. Cockrell Analysis and Design of Antennas for Air Traffic Collision Avoidance Systems, *IEEE Trans. Aerosp. Electron. Syst.*, September 1971, Vol. AES-7, pp. 960–967.
16. Balanis, C. A. Radiation from Conical Surfaces Used for High-Speed Aircraft, *Radio Sci.*, February 1972, Vol. 7, pp. 339–343.
17. Croswell, W. F., et al. The Admittance of a Rectangular Waveguide Radiating into a Dielectric Slab, *IEEE Trans. Antennas Propag.*, September 1967, Vol. AP-15, pp. 627–633.
18. Bailey, M. C., et al. Electromagnetic Properties of a Circular Aperture in a Dielectric Covered or Uncovered Groundplane, *NASA Langley Tech. Note* D-7452, October 1968.
19. Bailey, M. C., and C. T. Swift Input Admittance of a Circular Waveguide Aperture Covered by a Dielectric Slab, *IEEE Trans. Antennas Propag.*, July 1968, Vol. AP-16, pp. 386–391.
20. Balanis, C. A. Pattern Distortion Due to Edge Diffractions, *IEEE Trans. Antennas Propag.*, July 1970, Vol. AP-18, pp. 561–563.
21. Southworth, G. C., and A. P. King Metal Horns as Directive Receivers of Ultrashort Waves, *Proc. IRE*, 1939, Vol. 27, pp. 95–102.
22. Barrow, W. L., and L. J. Chu Theory of the Electromagnetic Horn. *Proc. IRE*, January 1939, Vol. 27, pp. 51–64.
23. Chu, L. J., and W. L. Barrow Electromagnetic Horn Design, *Trans. AIEE*, July 1939, Vol. 58, pp. 333–338.
24. Barrow, W. L., and F. D. Lewis The Sectoral Electromagnetic Horn, *Proc. IRE*, January 1939, Vol. 27, pp. 41–50.
25. Chu, L. J. Calculation of the Radiation Properties of Hllow Pipes and Horns, *J. App. Phys.*, 1940, Vol. 11, pp. 603–610.
26. Schelkunoff, S. A. "Electromagnetic Waves," Van Nostrand, 1943.
27. Rhodes, D. R. An Experimental Investigation of the Radiation Properties of Electromagnetic Horn Antennas, *Proc. IRE*, September 1948, Vol. 36, pp. 1101–1105.
28. Schelkunoff, S. A., and H. T. Friis "Antennas: Theory and Practice," Wiley, 1952.

29. King, A. P. The Radiation Characteristics of Conical Horn Antennas, *Proc. IRE*, March 1952, Vol. 38, pp. 249–251.
30. Schorr, M. G., and J. J. Beck Electromagnetic Field of the Conical Horn, *J. App. Phys.*, August 1950, Vol. 21, pp. 795–801.
31. Compton, R. T., Jr., and R. E. Collin Open Waveguides and Small Horns, in R. E. Collin and F. J. Zucker "Antenna Theory," Pt. I, pp. 621–655, McGraw-Hill, 1969.
32. Russo, P. M., R. C. Rudduck, and L. Peters A Method for Computing *E*-Plane Patterns of Horn Antennas, *IEEE Trans. Antennas Propag.*, March 1965, Vol. AP-13, pp. 219–224.
33. Yu, J. S., R. C. Rudduck, and L. Peters Comprehensive Analysis for *E*-Plane of Horn Antennas by Edge Diffraction Theory, *IEEE Trans. Antennas Propag.*, March 1966, Vol. AP-14, pp. 138–149.
34. Yu, J. S., and R. C. Rudduck *H*-Plane Pattern of a Pyramidal Horn, *IEEE Trans. Antennas Propag.*, September 1969, Vol. AP-17, pp. 651–652.
35. Thomas, D. T. A Half Blinder for Reducing Certain Side-Lobes in Large Horn, Reflector Antennas, *IEEE Trans. Antennas Propag.*, November 1971, Vol. AP-19, pp. 774–776.
36. Jull, E. V. Reflection from the Aperture of a Long *E*-Plane Sectoral Horn, *IEEE Trans. Antennas Propag.*, January 1972, Vol. AP-20, pp. 62–68.
37. Wrixom, G. T., and W. J. Welch Gain Measurements of Standard Electromagnetic Horns in the K and K_a Bands, *IEEE Trans. Antennas Propag.*, March 1972, Vol. AP-20, pp. 136–142.
38. Jakes, W. C. Horn Antennas, in H. Jasik (ed.), "Antenna Engineering Handbook," pp. 10-1 to 10–18, McGraw-Hill, 1961.
39. Mac A. Thomas, B. Design of Corrugated Conical Horns, *IEEE Trans. Antennas Propag.*, Vol. AP-26, No. 2, March 1978, pp. 698–703.
40. Simmons, A. J. and A. F. Kay "The Scalarfeed—A High-Performance Feed for Large Paraboloid Reflectors," Design and Construction of Large Steerable Aerials, *IEEE Conf. Pub. 21*, 1966, pp. 762–773.
41. Silver, S. "Microwave Antenna Theory and Design," M.I.T. Radiation Laboratory Series, Vol. 12, McGraw-Hill, 1949.
42. Gray, C. Larry Estimating the Effect of Feed Support Member Blocking on Antenna Gain and Sidelobe Level, *Microwave J*., March 1964, pp. 88–91.
43. Ruze, J. Lateral-Feed Displacement in a Paraboloid, *IEEE Trans. Antennas Propag.*, September 1965, Vol. AP-16, pp. 660–665.
44. Pagones, M. J. Gain Factor of an Offset-Fed Paraboloidal Reflector, *IEEE Trans. Antennas Propag.*, September 1965, Vol. AP-16, pp. 536–541.
45. Love, A. W. Spherical Reflecting Antennas with Corrected Line Sources, *IEEE Trans. Antennas Propag.*, September 1962, Vol. AP-13, pp. 529–537.
46. Schell, A. C. The Diffraction Theory of Large-Aperture Spherical Reflector Antennas, *IEEE Trans. Antennas Propag.*, July 1963, Vol. AP-14, pp. 428–532.
47. Potter, P. D. The Aperture Efficiency of Large Paraboloidal Antennas as a Function of Their Feed System Radiation Characteristics, *Jet Prop. Lab. Tech. Rep.* 32–149, September 25, 1961.
48. Rusch, W. V. T. Phase Error and Associated Cross-Polarization Effects in Cassegrainian-Fed Microwave Antennas, *Jet Prop. Lab. Tech. Rep.* 32-612, May 30, 1962.
49. Potter, P. D. The Application of the Cassegrainian Principle to Ground Antennas for Space Communications, *Jet Prop. Lab. Tech. Rep.* 32-295, June 1962.
50. Potter, P. D. A Simple Beamshaping Device for Cassegrainian Antennas, *Jet Prop. Lab. Tech. Rep.* 32-214, Jan. 31, 1962.
51. Potter, P. D. A Computer Program for Machine Design of Cassegrain Feed Systems, *Jet Prop. Lab. Tech. Rep.* 32-1202, December 15, 1967.
52. Rusch, W. V. T. Edge Diffraction from Truncated Paraboloids and Hyperboloids, *Jet Prop. Lab. Tech. Rep.* 32-113, June 1, 1967.
53. Ludwig, A., and W. T. T. Rusch Digital Computer Analysis and Design of a Subreflector of Complex Shape, *Jet Prop. Lab. Tech. Rep.* 32-1190, November 15, 1967.
54. Williams, W. F. High Efficiency Antenna Reflector, *Microwave J.*, July 1965, pp. 79–82.
55. Potter, P. D. Application of Spherical Wave Theory to Cassegrain-Fed Paraboloids, *IEEE Trans. Antennas Propag.*, November 1967, Vol. AP-15, pp. 727–736.

56. Space Program Summary, *Jet Prop. Lab. Tech. Rep.* 37-50, January 1, 1968-March 31, 1968.
57. The Deep Space Network, *Jet Prop. Lab. Space Programs Summ.* 37–52, Vol. II, July 31, 1968, pp. 78–105.
58. Meeks, M. L., and J. Ruze Evaluation of the Haystack Antenna and Radome, *IEEE Trans. Antennas Propag.*, November 1971, Vol. AP-19, pp. 723–728.
59. Ingerson, P. G., and W. C. Wong The Analysis of Deployable Umbrella Parabolic Reflectors, *IEEE Trans. Antennas Propag.*, July 1972, Vol. AP-20, pp. 409–415.
60. Ludwig, A. C. Conical-Reflector Antennas, *IEEE Trans. Antennas Propag.*, November 1972, Vol. AP-20, pp. 146–152.
61. Knop, C. M., "Microwave Relay Antenna, Chapter 31, Antenna Engineering Handbook," McGraw-Hill, 1993.
62. Rumsey, V. H. The Equiangular Spiral, *IRE Nat. Conv. Rec.*, 1957, Pt. I, pp. 114–118.
63. Dyson, J. D. The Equiangular Spiral, *IRE Trans. Antennas Propag.*, April 1959, Vol. AP-7, pp. 181–187.
64. Springer, P. S. End-Loaded and Expanding Helices as Broadband Circularly Polarized Radiators, *Proc. Natl. Electron. Conf.*, 1949, Vol. 5, pp. 161–171.
65. Chatterjee, J. S. Radiation Characteristics of a Conical Helix of Low Pitch Angles, *J. Appl. Phys.*, March 1955, Vol. 26, pp. 331–335.
66. Duhamel, R. H., and R. E. Isbell Broadband Logarithmically Periodic Antenna Structures, *IRE Natl. Conv. Rec.*, 1957, Pt. 1, pp. 119–128.
67. Dyson, J. D. The Unidirectional Equiangular Spiral Antenna, *IRE Trans. Antennas Propag.*, October 1959, Vol. AP-7, pp. 329–334.
68. Mayes, P. E., and R. L. Carrel Log-Periodic Resonant V-Arrays, *IRE West. Conv.*, 1961.
69. Isbell, D. E. Log-Periodic Dipole Arrays, *IRE Trans. Antennas Propag.*, May 1960, Vol. AP-8, pp. 260–267.
70. Carrel, R. L. The Design of Logarithmically Periodic Dipole Antennas, *IRE Natl. Conv. Rec.*, 1961, Pt. 1, pp. 61–75.
71. Barbano, N. Log-Periodic Yagi-Uda Array, *IEEE Trans. Antennas Propag.* March 1966, Vol. AP-14, pp. 235–238.
72. Mailloux, R. J. The Long Yagi-Uda Array, *IEEE Trans. Antennas Propag.* March 1966, Vol. AP-14, p. 128.
73. Collin, R. E. "Field Theory of Guided Waves," McGraw-Hil, 1960.
74. Brunstein, S. A., and R. F. Thomas Characteristics of a Cigar Antenna, *Jet Prop. Lab. Q. Rev.*, July 1972, Vol. 1, No. 2, pp. 87–95.
75. Zucker, F. J. Surface Wave Antennas, in R. E. Collin and F. J. Zucker (eds.), "Antenna Theory," Pt. II, Chap. 21, pp. 298-348, McGraw-Hill, 1969.
76. Zucker, F. J. Surface and Leaky-Wave Antennas, in H. Jasik (ed.), "Antenna Engineering Handbook," Chap. 16, pp. 16–1 to 16–57, McGraw-Hill, 1961.
77. Kraus, J. D. "Antennas," McGraw-Hill, 1950.
78. Angelakos, D. J., and Kajfez Darko Modifications on the Axial Mode Helical Antenna, *Proc. IEEE*, April 1967, Vol. 55, No. 4, pp. 558–559.
79. Carver, K. R., and B. M. Potts Some Characteristics of the Helicone Antenna, *1970 IEEE G-AP Symp. Dig.*, pp. 142–150.
80. Croswell, W. F., and M. C. Gilreath Erectable Yagi Disk Antennas for Space Vehicle Applications, *NASA Langley Tech. Note* D-1401, October 1962.
81. Lo, Y. T., D. Solomon, and W. F. Richards Theory and Experiment on Microstrip Antennas, IEEE *Trans. Antennas Propag.*, March 1979, Vol. AP-27, pp. 137–145.
82. Bailey, M. C. Resonant Frequency of Microstrip Antennas Calculated from TE-Excitation of an Infinite Strip Embedded in a Grounded Dielectric Slab, *NASA Langley Tech. Mem.* 80190, November 1979.
83. Derneryd, A. G. Linearly Polarized Micorstrip Antennas, *IEEE Trans. Antennas Propag.*, November 1976, Vol. AP-24, pp. 846–851.
84. Agrawal, P. K., and M. C. Bailey An Analysis Technique for Micorstrip Antennas, *IEEE Trans. Antennas Propag.*, November 1977, Vol. AP-25, pp. 756–759.
85. Carver, K. R. A Modal Expansion Theory for the Microstrip Antenna, *IEEE AP-S Symp. Dig.*, 1979, pp. 101–104.
86. Richards, W. F., and Y. T. Lo Am Improved Theory for Microstrip Antennas and Applications, *IEEE AP-S Symp. Dig.*, 1979, pp. 113–116.

87. Bailey, M. C., and F. G. Parks Design of Microstrip Disk Antenna Arrays, *NASA Langley Tech. Mem.* 78631. February 1978.

88. Hammer, P., D. Van Bauchaute, D. Verschraeven, and S. Van de Capelle A Model for Calculating the Radiation Field of Microstrip Antennas, *IEEE Trans. Antennas Propag.*, March 1979, Vol. AP-27, pp. 167–270.

89. Milligan, T. A., Modern Antenna Design, McGraw-Hill, 1985.